THE JOURNAL OF BIOLOGICAL CHEMISTRY VOL. 289, NO. 32, pp. 21995–22007, August 8, 2014

The Putative Exchange Factor Gef3p Interacts with Rho3p GTPase and the Septin Ring during Cytokinesis in Fission Yeast*[S]

Received for publication, January 8, 2014, and in revised form, June 16, 2014 Published, JBC Papers in Press, June 19, 2014, DOI 10.1074/jbc.M114.548792

Sofía Muñoz[1], **Elvira Manjón**[2], **and Yolanda Sánchez**[3]

From the Instituto de Biología Funcional y Genómica (IBFG), Consejo Superior de Investigaciones Científicas and Departamento de Microbiología y Genética, Universidad de Salamanca, C/ Zacarías González, s/n. 37007 Salamanca, Spain

Background: Guanine nucleotide exchange factors (GEFs) regulate the activity of small GTPases to control cellular functions.
Results: Gef3p interacts with the GTPase Rho3p at the division site and localizes to the septin ring.
Conclusion: The module Gef3p/Rho3p contributes to downstream events in the secretory pathway.
Significance: The interactions between septins and Rho-GEFs provide a new targeting mechanism for GTPases to direct secretion in cytokinesis.

The small GTP-binding proteins of the Rho family and its regulatory proteins play a central role in cytokinetic actomyosin ring assembly and cytokinesis. Here we show that the fission yeast guanine nucleotide exchange factor Gef3p interacts with Rho3p at the division site. Gef3p contains a putative DH homology domain and a BAR/IMD-like domain. The protein localized to the division site late in mitosis, where it formed a ring that did not constrict with actomyosin ring (cytokinetic actomyosin ring) invagination; instead, it split into a double ring that resembled the septin ring. Gef3p co-localized with septins and Mid2p and required septins and Mid2p for its localization. Gef3p interacts physically with the GTP-bound form of Rho3p. Although Gef3p is not essential for cell separation, the simultaneous disruption of *gef3*$^+$ and Rho3p-interacting proteins, such as Sec8p, an exocyst component, Apm1p, a subunit of the clathrin adaptor complex or For3p, an actin-polymerizing protein, yielded cells with strong defects in septation and polarity respectively. Our results suggest that interactions between septins and Rho-GEFs provide a new targeting mechanism for GTPases in cytokinesis, in this case probably contributing to Rho3p function in vesicle tethering and vesicle trafficking in the later steps of cell separation.

Cytokinesis is the final step in the process of cell division, during which two daughter cells are generated. From animal to fungal cells, cytokinesis requires coordinated contractile actomyosin ring closure and plasma membrane extension (1, 2). In addition, fungal cytokinesis requires the synthesis of a special division wall termed septum. Cells of the fission yeast *Schizosaccharomyces pombe* are rod-shaped and divide by medial fission. In *S. pombe* cells, cytokinesis starts at late anaphase, triggered by activation of the septation initiation network that promotes contractile actomyosin ring constriction and plasma membrane ingression (3). Both processes guide the deposition of a multilayered division septum composed of a middle disk, called the primary septum, covered on both sides by the secondary septum (4–6). The last step in cytokinesis is cell separation by controlled cell-wall and primary septum degradation. Correct septum formation, and especially cell separation, are critical processes for cell integrity and survival and must be tightly restricted in space and time (7, 8).

Guanine nucleotide-exchange factors (GEFs)[4] of the Rho family are key proteins in the process of cytokinesis in mammals and budding yeast (9–11). GEFs are responsible for the activation of Rho-family GTPases in response to diverse stimuli; GEFs are much larger and complex proteins than the GTPases themselves, and they contain protein-protein interaction domains that could be important for GTPase localization, activation, stabilization, and interaction with their effectors (12–15).

S. pombe contains eight proteins with a Rho-GEF domain (Scd1p, Gef1p, Gef2p, Gef3p, Rgf1p, Rgf2p, Rgf3p, and Mug10p) (16–18) and six Rho GTPases (Cdc42p and Rho1p, Rho2p, Rho3p, Rho4p, and Rho5p). Scd1p and Gef1p are Cdc42p-specific GEFs. Gef1p and Scd1p form a ring structure at the cell division site that shrinks during cytokinesis after contraction of the contractile actomyosin ring. Both Scd1p and Gef1p collaborate in the recruitment of active Cdc42p to the septation site (19, 20). Gef2p is involved in division-site and contractile-ring positioning by interacting with the anillin-re-

* This work was supported by Grants BFU2008-00963/BMC and BFU2011-24683/BMC from the Comisión Interministerial de Ciencia y Tecnología, Spain and GR231 from the Junta de Castilla y León.
[S] This article contains supplemental Movies 1 and 2.
[1] Supported by Consejo Superior de Investigaciones Científicas, Spain, Fellowship JAE-PreDoc.
[2] Supported by a contract from the Junta de Castilla y León and the Fondo Social Europeo.
[3] To whom correspondence should be addressed: Instituto de Biología Funcional y Genómica, CSIC/Universidad de Salamanca, C/Zacarías González s/n. 37007 Salamanca. Spain. Tel.: 34-923-294887; Fax: 34-923-224876; E-mail: ysm@usal.es.

[4] The abbreviations used are: GEF, guanine nucleotide-exchange factor; IBFG, Instituto de Biología Funcional y Genómica; YES, yeast growth medium; Cfw, Calcofluor; RBD, rhotekin-binding domain; nt, nucleotide(s); RFP, red fluorescent protein; BAR, Bin1/amphiphysin/Rvs167; IMD, IRSp53, and MIM (missing in metastases) homology domain.

lated protein Mid1p (21). Rgf1p, Rgf2p, and Rgf3p function as GEFs for Rho1p (the regulatory subunit of (1,3)-β-D-glucan synthase). Although Rgf1p and Rgf2p localize to the septum area, to date it has not been shown whether they play a role in cell division (22–25). Rgf3p activates Rho1p specifically in cytokinesis; it localizes exclusively to the middle region of the cell and is essential for maintaining cell integrity during cell separation (25–27). Gef2p, Gef3p, and Mug10p have not been assigned to any known GTPase, and the functions of Gef3p and Mug10p are unknown.

In this study we observed that a putative Rho-GEF, Gef3p, interacted physically with Rho3p. In fission yeast Rho3p has been isolated as a multicopy suppressor of *sec8-1*, a mutant allele of a component of the exocyst complex (28). The exocyst is highly conserved from yeasts to mammals and is involved in the late stages of exocytosis by targeting and tethering post-Golgi vesicles to the plasma membrane (29, 30). In *S. pombe*, mutations in exocyst components show defects in cell separation (28, 31, 32). Rho3p restored exocyst localization in a *cdc42* thermosensitive mutant with multiple membrane traffic defects (33), and it has been implicated in the regulation of Golgi/endosome trafficking through a functional interaction with adaptin (clathrin-associated adaptor protein-1) and Sip1p (34, 35). Thus, it is possible that Rho3p could stimulate secretion by locally increasing the exocytic apparatus or through Golgi/endosome regulation.

In addition, Rho3p has been implicated in polarized cell growth through both formin For3p (36) and Pob1p function (37). For3p and Pob1p mediate the formation of the actin cables that serve as tracks for the type V myosin-dependent delivery of secretory vesicles to sites of growth (37–40). Here we report that Gef3p interacts physically and functionally with Rho3p and plays a role during cytokinesis. In addition, Gef3p localization to the septin ring might provide a scaffold for septin-mediated Rho3p-directed polarized secretion during septum formation and cell separation.

EXPERIMENTAL PROCEDURES

Media, Reagents, and Genetics—The genotypes of the *S. pombe* strains used in this study are listed in Table 1. The complete yeast growth medium (YES), selective medium (MM) supplemented with the appropriate requirements, and sporulation medium (MEA) have been described elsewhere (41). Crosses were performed by mixing appropriate strains directly on MEA plates. For overexpression experiments using the *nmt1* promoter, cells were grown in selective medium (MM) containing 15 μM thiamine up to the logarithmic phase. Then the cells were harvested, washed 3 times with water, and inoculated in fresh medium without thiamine (−T) at an $A_{600} = 0.01$ for 16, 18, or 22 h, depending on the experiment.

Disruption of the gef3$^+$ Gene—The *gef3*::*ura4*$^+$ disruption construct was obtained in a two-step process. The 5′ non-coding region of the *gef3*$^+$ open reading frame (ORF) (nucleotides (nt −1584 to −40)) was amplified by PCR, inserting the ApaI and SalI sites (one at each end), and was ligated into the same sites of the SK-*ura4*$^+$ vector. The 3′ flanking region of the *gef3*$^+$ ORF (nt +1609 to +3577) was amplified by PCR, inserting the PstI and NotI sites as above, and was cloned into the same sites of pSK-*ura*$^+$ with the 5′ end to yield pSM31. *gef3*$^+$ gene disruption was accomplished using the 5.2-kb fragment from pSM31 cut with ApaI and NotI and transforming the YS64 haploid strain. Correct deletion of the *gef3*$^+$ ORF was confirmed by PCR analysis using oligonucleotides: M13 (5′-CTGGTGGCCTTAGGTAA-3′) in the *ura4*$^+$ gene and Gef3-Ext-5′ (5′-CTCCTAAGAAGCGGGAAG-3′) upstream from nucleotide +1153 and hence external to the disruption cassette.

Plasmid and DNA Manipulations—To make pAL*gef3*$^+$ (pPB7), the *gef3*$^+$ ORF was obtained from two PCR fragments; a BglII-PstI fragment (nt −80 to +1170) and a PstI-SmaI fragment (nt +1170 to +1645); both fragments were cloned into the same sites of pSM31 (described above) to make pPB7. The *gef3*$^+$ ORF was confirmed by the sequencing of four different clones of pPB7. To tag Gef3p at the N terminus with enhanced green fluorescent protein (GFP) (engineered with eight alanines at the C terminus) and with tdTomato (Cherry variant; Ref. 42), pAL-*gef3*$^+$ (pPB7) was modified by site-directed mutagenesis. The NotI site at the multiple cloning sites was destroyed, and site-directed mutagenesis was used to create a NotI site just before the ATG codon (pSM70). The GFP and tdTomato epitopes were inserted in-frame at the NotI site of pSM70 to create pSM71 and pSM74, respectively. Strains with a genomic copy of *gef3*$^+$ tagged with GFP or tdTomato were obtained by one-step gene replacement. pSM71 and pSM74 were modified to create a XhoI and a BamHI restriction site (nt −1220) before the promoter of the corresponding tagged version of the *gef3*$^+$ ORF, allowing the insertion of the *ura4*$^+$ marker at those sites and thus creating pSM86 and pSM87, respectively. An ApaI-XbaI cassette from pSM86 and pSM87 were used to transform strain YS64, respectively, creating the SM217 (GFP-*gef3*$^+$) and SM263 (tdTomato-*gef3*$^+$) strains. In addition, pSM89 and pSM90 were created, both containing cassettes (KanMX6-GFP-*gef3*$^+$) and (KanMX6-tdTomato-*gef3*$^+$) for kanamycin selection of the tagged *gef3*$^+$. For *gef3*$^+$ and GFP-tagged *gef3*$^+$ overexpression, pPB7 (pAL-*gef3*$^+$) and pSM71 (pAL-GFP-*gef3*$^+$) were modified by site-directed mutagenesis, introducing XhoI and SmaI sites flanking the *gef3*$^+$ ORF. The resulting XhoI-SmaI fragments were cloned into the same sites of pREP3x, thus affording pREP3x-*gef3*$^+$ and pREP3x-GFP-*gef3*$^+$. The strain with GFP-Rho3p tagged at the N terminus and plasmid pREP4x-GST-*rho3*$^+$ were kindly provided by P. Perez (Instituto de Biología Funcional y Genómica (IBFG), Salamanca, Spain). pREP4x-GST-*rho3*$^+$ was modified by site-directed mutagenesis to replace glycine 22 by valine, creating pREP4x-GST-*rho3*$^+$G22V.

Microscopy and Image Analysis—Cell samples were visualized using an Olympus IX71 microscope equipped with a personal Delta Vision system and a Photometrics CoolSnap HQ2 monochrome camera. Stacks of seven z-series sections were acquired at 0.2-μm intervals. All fluorescence images are maximum two-dimensional projections of z-series and were analyzed using deconvolution software from Applied Precision. Measurements were made from micrographs using the IMAGEJ (National Institutes of Health) or METAMORPH (Molecular Devices) programs. For Calcofluor (Cfw), cells were harvested (1 ml), washed once, and resuspended in water with 20 μg/ml Cfw at room temperature. For time-lapse imaging,

TABLE 1

***S. pombe* strains used in this work**

All strains were generated in this study except as indicated in the footnotes.

Strains	Genotypes
YS64	h$^-$ *leu1-32 ade6M210 ura4D-18 his3D1*
SM116	h$^-$ *gef3::ura4$^+$ leu1-32 ade6M210 ura4D-18 his3D1*
NG69	h$^-$ *cdc25-22 leu1-32 ura4D18*
SM176	h$^-$ *gef3::ura4$^+$ cdc25-22 leu1-32 ura4D18*
PG153[a]	h$^+$ *gef1::kanMX6 leu1-32 ura4D18*
SM143	h$^-$ *gef3::ura4$^+$ gef1::kanMX6 leu1-32 ura4D18*
CL5	h$^-$ *gef2::ura4$^+$ leu1-32 ade6M210 ura4D-18 his3D1*
SM172	h$^-$ *gef2::ura4$^+$ gef3::his3$^+$ leu1-32 ade6M210 ura4D-18 his3D1*
PG154[a]	h$^+$ *scd1::kanMX6 leu1-32 ura4D18*
SM157	h$^-$ *gef3::ura4$^+$ scd1::kanMX6 leu1-32 ura4D18*
VT14	h$^-$ *rgf1::his3$^+$ leu1-32 ade6M210 ura4D18 his3d1*
SM148	h$^-$ *gef3::ura4$^+$ rgf1::his3$^+$ leu1-32 ade6M210 ura4D1 his3d1*
PG1	h$^-$ *rgf2::ura4$^+$ his3d1 ura4D18 leu1-32 ade6M210*
SM150	h$^-$ *gef3::ura4$^+$ rgf2::ura4$^+$ his3d1 ura4D18 leu1-32 ade6M210*
MS264	h$^-$ *ehs2–1 leu1-32 ura4D18*
SM152	h$^-$ *gef3::ura4$^+$ ehs2–1 leu1-32 ura4D18*
SM217	h$^-$ *ura4$^+$:GFP-gef3$^+$ leu1-32 ura4D18*
SM267	h$^-$ *GFP-gef3:KanMX6 rlc-tdTomato:natMX6 ura4D18*
SM263	h$^-$ *ura4$^+$:tdTomato-gef3$^+$ leu1-32 ura4D18*
PPG2772[a]	h$^-$ *spn3-GFP:kanMX6 leu1-32 ade6M210 ura4D-18 his3D1*
SM197[b]	h$^-$ *mid2-GFP:kanMX6 leu1-32 ura4D-18*
SM297	h$^-$ *spn3-GFP:kanMX6-tdTomato gef3:ura4$^+$ leu1-32 ura4D-18*
SM295	h$^-$ *mid2-GFP:kanMX6 tdTomato-gef3:ura4$^+$ leu1-32 ura4D-18*
SM277[c]	h$^-$ *GFP-gef3:KanMX6 spn1–5::ura4$^+$ura4D18*
SM253	h$^-$ *GFP-gef3:KanMX6 mid2::ura4$^+$ ura4D18 leu1-32*
SM273	h$^-$ *spn3-GFP:kanMX6 gef3::ura4$^+$ leu1-32 ade6M210 ura4D-18 his3D1*
SM229	h$^-$ *mid2-GFP:kanMX6 gef3::ura4$^+$ leu1-32 ura4D-18*
SM271	h$^-$ *GFP-gef3:ura4$^+$ exo70-RFP:kanMX6 leu1-32 ura4D18*
SM259	h$^-$ *GFP-gef3:KanMX6 exo70::ura4$^+$ ura4D18 leu1-32*
SM261	h$^-$ *GFP-gef3:KanMX6 sec8–1 ura4D18 leu1-32*
MBY797[b]	h$^-$ *sec6-GFP:ura4$^+$ leu1-32 ura4D18*
MBY856[b]	h$^-$ *sec8-GFP:ura4$^+$ leu1-32 ura4D18*
SM244	h$^-$ *sec6-GFP:ura4$^+$ gef3::KanMX6 leu1-32 ura4D18*
SM245	h$^-$ *sec8-GFP:ura4$^+$ gef3::KanMX6 leu1-32 ura4D18*
SM242[a]	h$^-$ *kanMX6-GFP-rho3$^+$ leu1-32 ura4D18*
SM594	h$^-$ *kanMX6-GFP-rho3$^+$ gef3::ura4$^+$ leu1-32 ura4D18*
PPG3740[a]	h$^+$ *rho3::ura4$^+$ leu1-32 ade6M210 ura4D18*
EM257	h$^-$ *rho3::ura4$^+$ gef3::KanMX6 leu1-32 ade6M210 ura4D18*
SM686	h$^-$ *kanMX6-GFP-rho3$^+$ sid4-RFP:natMX6 leu1-32 ura4D18*
EM83[a]	h^{90} *leu1:GFP-Psy1*
EM256	h$^-$ *GFP-Psy: leu gef3::KanMX6*
MBY919[b]	h$^-$ *exo70::ura4$^+$ leu1-32 ura4D-18*
SM243	h$^-$ *exo70::ura4$^+$ gef3::KanMX6 leu1-32 ura4D-18*
MBY887[b]	h$^+$ *sec8–1 leu1-32 ura4D18*
SM226	h$^-$ *sec8–1 gef3::ura4$^+$ leu1-32 ura4D18*
PPG2567[a]	h$^-$ for3::*KanMX1 leu1-32 ura4D18*
SM300	h$^-$ for3::*KanMX1 gef3::ura4$^+$leu1-32 ura4D18*
SM708[d]	h$^-$ *apm1::ura4$^+$ leu1-32 ura4D18*
SM721	h$^-$ *gef3::KanMX6, apm1::ura4$^+$ leu1-32*

[a] From P. Pérez, IBFG, University of Salamanca.
[b] From C. R. Vázquez de Aldana, IBFG, University of Salamanca.
[c] From J. Bähler, Wellcome Trust, UK.
[d] From H. Valdivieso, IBFG, University of Salamanca.

0.3–0.6 ml of log-phase cells were collected by low speed centrifugation (3000 × *g* for 1 min), suspended in 0.3 ml of YES media containing Cfw (5 μg/ml final concentration), and placed in a well from a μ-Slide 8 well (80821-Uncoated; Ibidi) previously coated with 10 μl of 1 mg/ml soybean lectin (L1395; Sigma).

Yeast Two-hybrid Analysis—For two-hybrid screenings, the entire ORF of *gef3*$^+$ w/o intron was modified to introduce BamHI and NcoI flanking sites and was cloned into the same sites of pGADT7 (Clontech) to express the GAL4-activating domain fused to the Gef3p (pSM73). GTPases *rho1*$^+$ to *rho5*$^+$ and *cdc42*$^+$ cloned into pAS2 were kindly provided by Perez and P. M. Coll (IBFG, Salamanca, Spain) (43) and were used as bait against *gef3*$^+$. The *Saccharomyces cerevisiae* AH109 strain, which carries the GAL4 recognition sequence and the *lacZ* and *HIS3* reporter genes, was transformed with different combinations of plasmids.

GST Pulldown Assay—For Gef3p/Rho3p GST pulldown assays, the wild-type strain expressing pAL-GFP-*gef3*$^+$ (pSM107) was transformed with either pREP4x-GST, pREP4x-GST-*rho3*$^+$, or pREP4x-GST-*rho3*$^+$ G22V (pSM139). Rho3 protein expression was induced by growing the cells in the absence of thiamine for 15 h at 28 °C. Cell homogenates from 50-ml cultures (absorbance = 0.6) were obtained using 200 μl of lysis buffer (50 mM HCl-Tris, pH 7.5, 200 mM NaCl, 2 mM EDTA, 0.5% Nonidet P-40, containing 1 mM *p*-amino phenylmethanesulfonyl fluoride, 1 μg/ml leupeptin, 1 μg/ml aprotinin, and 1 μg/ml pepstatin). Extracts were cleared by centrifugation at 2500 × g for 5 min, and ~1 mg of total protein was used in each immunoprecipitation in a final volume of 600 μl. The extracts were incubated with 20 μl of glutathione-Sepharose beads for 2 h at 4 °C in immunoprecipitation buffer (same as the lysis buffer w/o Nonidet P-40 and with 2% Triton X-100 instead). The beads were washed 3× with immunoprecipita-

tion buffer and 1× with immunoprecipitation buffer containing 500 mM NaCl and then resuspended in sample buffer and separated by 4–12% SDS-PAGE (Invitrogen). Proteins were transferred electrophoretically to an Immobilon-P membrane (Millipore, Bedford, MA) and blotted with α-GFP antibody JL-8 (BD Living Colors) to detect *GFP-Gef3p* and with conjugated anti-GST-HRP (Amersham Biosciences) to detect GST-Rho3p. Total protein levels were monitored in whole-cell extracts (10 μg of total protein) and used directly for Western blots.

Pulldown Assays for GTP-bound Rho Proteins—The GST-rhotekin binding domain (RBD) fusion protein was obtained as described previously (24). The amount of GTP-bound Rho proteins was analyzed using the Rho-GTP pulldown assay, modified as described in Ren *et al.* (44). Extracts from 50-ml cultures of cells expressing pREP3X-HA*rho3*$^+$ transformed with pREP4X-HA*gef3*$^+$ or the empty plasmid grown for 18 h in minimal medium (−T) were obtained using 200 μl of lysis buffer (50 mM Tris, pH 7.5, 20 mM NaCl, 0.5% Nonidet P-40, 10% glycerol, 0.1 mM dithiothreitol, 2 mM $MgCl_2$, containing 100 μM *p*-amino phenylmethanesulfonyl fluoride, leupeptin, and aprotinin). 100 μg of GST-RBD fusion protein coupled to glutathione-agarose beads was used to immunoprecipitate 1.5 mg of the cell lysates. The extracts were incubated with GST-RBD beads for 2 h at 4 °C. The beads were washed with lysis buffer four times, and bound proteins were blotted against 1:5000-diluted 12CA5 mAb as the primary antibody to detect HA-Rho3p. The total amount of HA-Rho3p was monitored in whole-cell extracts (10 μg of total protein) by Western blot with 12CA5 mAb. Immunodetection was accomplished using the ECL detection kit (Amersham Biosciences).

RESULTS

*gef3*Δ *Mutant Cells Show Defects in Cell Separation*—Gef3p was first reported as a GEF by Iwaki *et al.* (17). Gef3p contains a DH homology domain, also called the Rho-GEF domain, at amino acids 68–273, and a BAR/IMD-like domain at amino acids 387–495, present in proteins involved in membrane dynamics (Fig. 1*A*). BAR (Bin1/amphiphysin/Rvs167) domains have been characterized by their function in sensing and inducing membrane curvature, but they are also involved in binding to small GTPases (45, 46). To investigate the role of Gef3p in the control of morphology, we deleted *gef3*$^+$ by replacing the *gef3*$^+$ ORF with the *ura4*$^+$ marker. The *gef3*Δ mutant grew well under standard growth conditions at both 28 and 37 °C and entered the stationary phase at the same time as the wild-type cultures. *gef3*Δ cells did not exhibit any evident morphological changes as judged by light microscopy (17) (Fig. 1*B*), but in asynchronous cultures ~25% of the cells in the *gef3*Δ mutant showed a septum compared with only 18% of the cells in the wild-type strain (Fig. 1*C*). To examine septation in more detail, we constructed the double mutant *cdc25-22 gef3*Δ and synchronized cells in G_2 by *cdc25-22* arrest and release. In both strains septation peaked after ~80 min, but the septation index remained high in *cdc25-22 gef3*Δ cells as compared with the wild-type *cdc25-22* cells (Fig. 1*D*). This suggested that septum formation proceeds normally, but cell separation is slower in the absence of Gef3p.

We then wondered whether there was a functional relationship between Gef3p and the other known GEF proteins in fission yeast. Curiously, the septation defect of the cells deleted for *gef3*$^+$ was exacerbated when combined with a deletion in *gef1*$^+$ and *gef2*$^+$ (Fig. 1*E*). No interaction was seen when combined with null mutations in Scd1p, Rgf1p, and Rgf2p, but we detected a positive interaction with the *ehs2-1* mutant (a point mutation in the *rgf3*$^+$ gene) (27). Deletion of Gef3p suppressed the growth defect of *ehs2-1* cells in the presence of NaF and strongly diminished the number of lysed cells in the *ehs2-1* mutant grown at 37 °C (Fig. 1*F*). The *gef1*, *gef2*, and *ehs2-1* mutants showed defects in cytokinesis, further suggesting that Gef3p is involved in this process.

Gef3p Localizes as a Ring That Splits and Persists until the End of Septation—To determine the intracellular location of Gef3p, we replaced the chromosomal *gef3*$^+$ ORF with the GFP gene and an eight-alanine linker fused in-frame to either the 5′ end or the 3′ end of *gef3*$^+$. Cells carrying the GFP at the N terminus were morphologically normal and behaved like the wild type in combination with *gef1*Δ mutants, indicating that the fusion protein was functional. However, we were unable to visualize the protein tagged at the C-end, suggesting that the BAR/IMD-like domain is required for the proper localization of Gef3p (not shown). GFP-Gef3p was detected at the division site in cells undergoing cytokinesis (Fig. 2*A*; the cells were synchronized to show a high proportion of septated cells). To determine whether Gef3p assembles into a ring structure, we used confocal microscopy and acquired Z sections of cells expressing GFP-Gef3p. The reconstruction of these images in Fig. 2*B* reveals that Gef3p indeed formed a ring structure; however, we were unable to observe rings of different diameters in cells undergoing cytokinesis (supplemental Movies 1 and 2). To determine the localization pattern of Gef3p during ring contraction, a GFP-Gef3p Rlc1p-tdTomato strain was constructed. The myosin regulatory light chain Rlc1p-tdTomato was used as a marker of contraction (47). The images show that GFP-Gef3p assembled into a ring structure, and both proteins colocalized at the end of mitosis (Fig. 2*C*, *cell 6*), but whereas Rlc1p-tdTomato constricted during septation, most of the GFP-Gef3p remained static until the end of cytokinesis (Fig. 2*C*, *cells 1* and *2*).

We next analyzed the localization of GFP-Gef3 by time-lapse microscopy in cells stained with Cfw, a dye used to track septum assembly and cell separation in *S. pombe* cells (48). The time-lapse images revealed that GFP-Gef3p concentrated in a ring detected concomitantly with the appearance of the primary septum (Fig. 2*D*, *cells 1* and *2 with yellow arrow*, time 27 and 15 min, respectively). As the septum formed, the GFP-Gef3p ring split into a double ring that persisted along septation and was dissipated after cell cleavage (see enlarged cells and cell 2 marked with a *yellow arrow* in Fig. 2*D*). Thus, these data indicate that Gef3p localizes to the division site as a double ring during the later stages of cytokinesis.

Gef3p Colocalizes with Mid2p and Septins and Is Dependent on Mid2p and Septins for Localization—In fission yeast septins appear at the division site, where they form a ring that splits as the septum forms, and this ring does not constrict with actomyosin ring invagination (49–51). The similarities with Gef3p

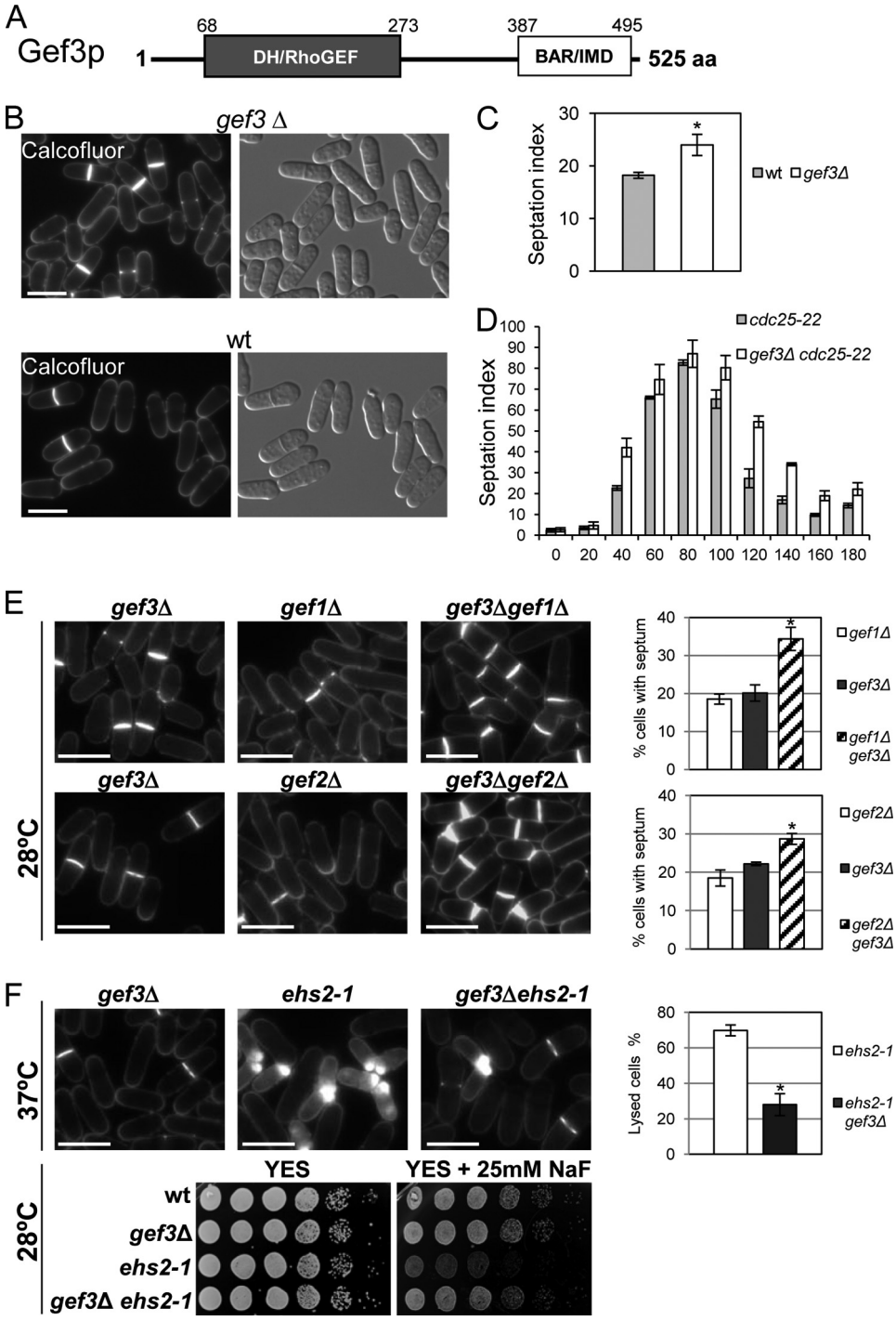

FIGURE 1. **gef3Δ mutant cells show defects in cell separation.** *A*, schematic representation of the domain structure of Gef3p. The *numbers* indicate amino acids, beginning with the start methionine. *DH/RhoGEF*, Dbl-homology domain; *BAR/IMD*, BAR-like homology domain. *aa*, amino acids. *B*, morphology of *gef3*Δ null cells. Cfw staining and differential interference contrast micrographs of *S. pombe gef3*Δ (SM116) and wild-type (YS64) cells grown in YES liquid medium at 28 °C. *Bar*, 10 μm. *C*, asynchronous cultures of wild-type and *gef3*Δ cells growing exponentially were stained with Cfw. The septation index is the percentage of septated cells in the culture and was quantified directly by fluorescence microscopy ($n = 200$). Values are the means from three independent experiments, and S.D. *bars* are indicated. The *asterisk* indicates that the *gef3*Δ value is significantly ($p < 0.05$) different from that of the wild type. *D*, cultures of *cdc25-22* (NG69) and *gef3*Δ *cdc25-22* (SM176) were synchronized in early G_2 and released into mitosis. The septation index was quantified as in *C* at the indicated times (minutes). *E*, *ef3*Δ (SM176), *gef1*Δ (PG153), *gef3*Δ *gef1*Δ (SM143), *gef2*Δ (CL5), and *gef3*Δ *gef2*Δ (SM172) cells growing exponentially were stained with Cfw to visualize septa. *Bar*, 10 μm. The *graphs on the right* represent the septation index of each set of mutants (the double mutant and the parental strains). At least 200 cells were scored in three independent experiments. Mean values were plotted with *error bars* representing the S.D. around the mean. *, $p < 0.01$ *versus gef3*Δ. *F*, loss of Gef3p reduces the lysis and abolishes the sensitivity to NaF of the *ehs2-1* (*rgf3*) mutant. *gef3*Δ (SM176), *ehs2-1*(MS264), and *gef3*Δ*ehs2-1* (SM152) cells were stained with Cfw. The graphic represents the percentage of lysis of *ehs2-1* and *gef3*Δ*ehs2-1* cell growth for 4 h at 37 °C. The NaF hypersensitivity of wild type, *gef3*Δ, *ehs2-1*, and *gef3*Δ*ehs2-1* was analyzed on a plate assay. Cells were spotted onto YES plates with or without 25 mM NaF as serial dilutions (8×10^4 cells in the *left row* and then 4×10^4, 2×10^4, 2×10^3, 2×10^2, and 2×10^1 in each subsequent spot) and incubated at 28 °C for 3 days. *, $p < 0.01$ *versus ehs2-1*.

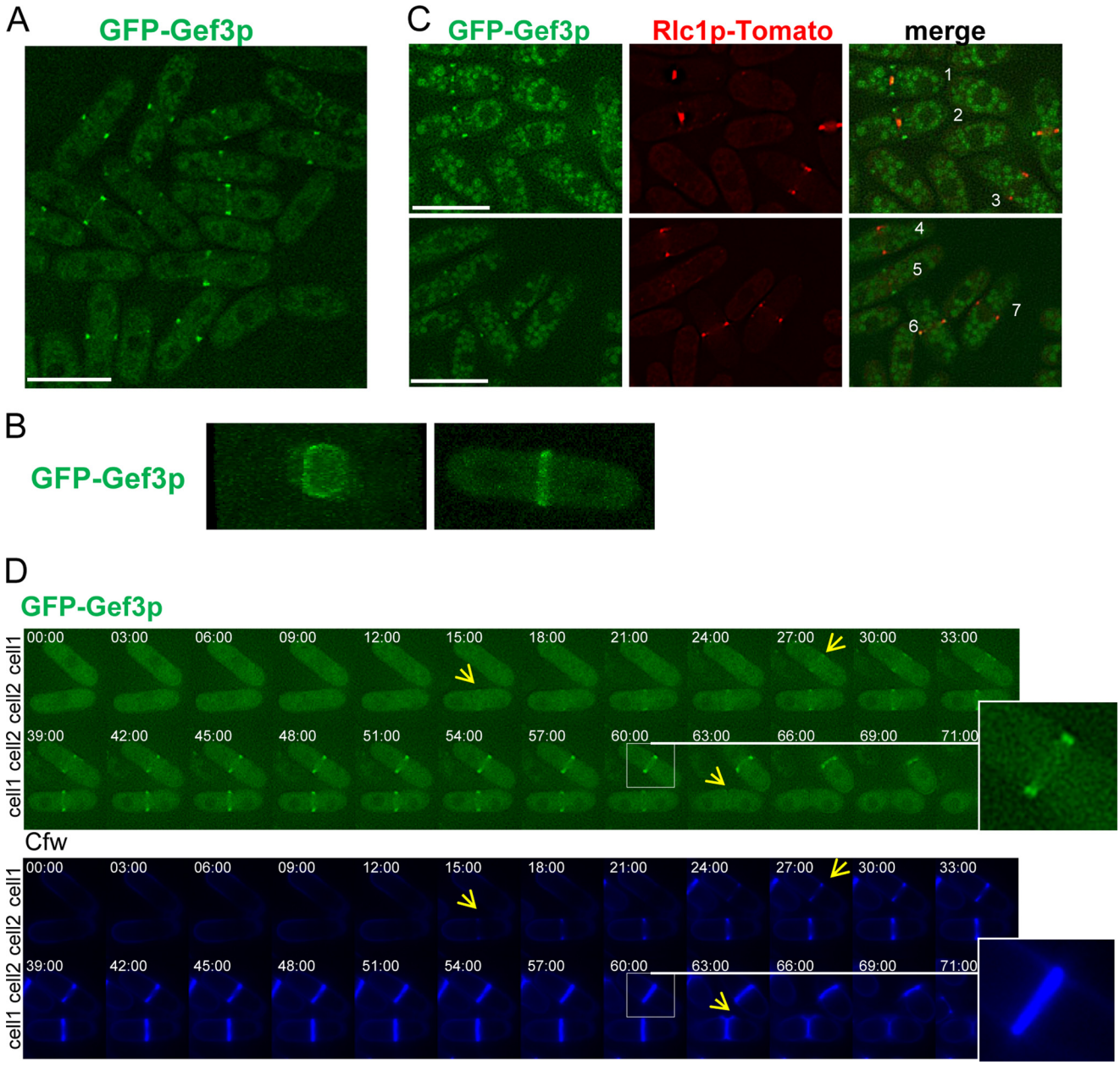

FIGURE 2. **Gef3p localizes as a medial ring.** *A*, cells producing GFP-Gef3p (SM217) were synchronized with 12.5 mM hydroxyurea (*HU*) for 2.5 h, washed 3*x*, and photographed 1 h after release into fresh medium. *Bar*, 10 μm. *B*, cells expressing GFP-Gef3p were imaged for GFP fluorescence using confocal three-dimensional microscopy. Frontal and lateral views of the GFP-Gef3p septum are shown (see supplemental Movies 1 and 2). *C*, cells (SM267) expressing GFP-Gef3p and Rlc1p-tdTomato were imaged for GFP and RFP fluorescence. During ring contraction, most Gef3p remains as an external ring (*cells 1* and *2*). *Cells 3*, *4*, and *7* exhibit myosin but not Gef3p staining, whereas *cell 5* shows just the opposite. *Bar*, 10 μm. *D*, *GFP-gef3*$^+$ cells were imaged by time-lapse microscopy. The elapse time is shown in minutes. The *inset* shows that the GFP-Gef3p ring splits into a double ring.

prompted us to analyze a possible relationship between the septins and Gef3p. First, we studied the localization of both proteins in the same cell using a strain that simultaneously expressed Spn3p-GFP and Tomato-Gef3p. We found that Gef3p and Spn3p colocalized during septation (Fig. 3*A*). Curiously, in >100 cells scored we did not find cells with Tomato-Gef3p present and Spn3p-GFP absent. This result suggests that Spn3p may precede Gef3p localization at the medial ring. Colocalization experiments with Mid2p-GFP (a protein necessary for proper organization of the septin ring) provided similar results (Fig. 3*B*). We also tested the dependence of Gef3p localization on septins and Mid2p. In *mid2*Δ cells and *spn1–5*Δ cells, GFP-Gef3p was not localized to any specific structure (Fig. 3*C*). A Western blot revealed that GFP-Gef3p was expressed in both mutants (Fig. 3*D*). As expected, Mid2p and the septins localized normally in *gef3*Δ cells (not shown). Thus, the results concerning the order and the localization dependence suggest that Gef3p associates with the septin ring for proper localization.

The exocyst is a multiprotein complex involved in polarized exocytosis (52). In fission yeast, the exocyst localizes to a double ring at the site of cell constriction; it is essential for cell separation, and its function is modulated by Rho3p (28, 37). Thus, as above we analyzed the localization of Gef3p-GFP and Exo70-RFP in the same cells. Gef3p localization coincided with that of

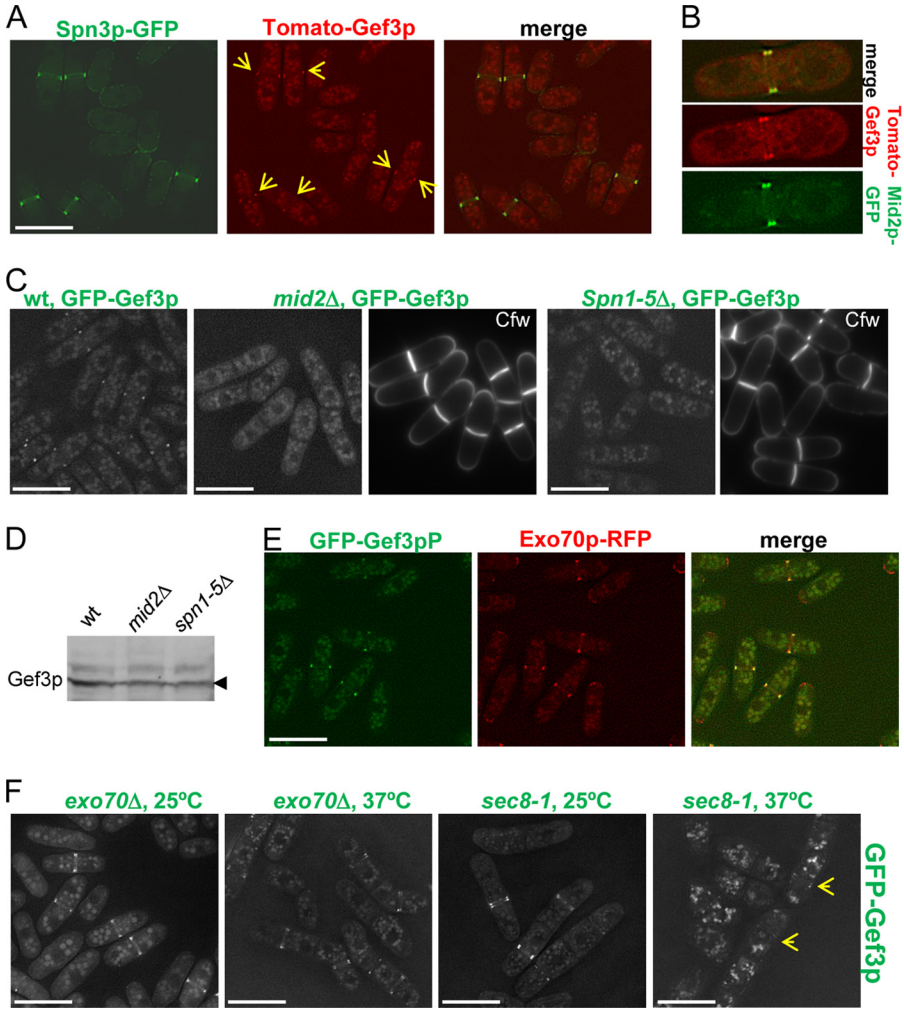

FIGURE 3. **Gef3p colocalizes with septins and Mid2p and its localization is dependent on septins and Mid2p.** *A*, Spn3p and Gef3p colocalize during septum formation. SM297 cells expressing Spn3p-GFP (*green*) and tdTomato-Gef3p (*red*) were imaged for GFP and RFP fluorescence. *B*, cells (SM295) expressing Mid2p-GFP and tdTomato-Gef3p colocalize in a double ring structure. *C*, Gef3p localization in septin ring mutants. Wild-type, *mid2*Δ, and *spn1–5*Δ mutants expressing GFP-Gef3p (SM217, SM253, and SM277, respectively) were treated with Cfw to visualize the septum and imaged for GFP and Cfw fluorescence. *D*, the amount of GFP-Gef3p expressed from the chromosome in wild type, *mid2*Δ, and *spn1–5*Δ mutants. Gef3p levels were measured with Western blots using anti-GFP antibodies. *E*, Gef3p colocalizes with the exocyst. Wild-type cells expressing GFP-Gef3p and Exo70p-RFP (SM259) were imaged for GFP and RFP fluorescence. *F*, Gef3p localization in exocyst mutants. *exo70*Δ (*left*) and *sec8-1* (*right*) mutants expressing GFP-Gef3p (SM259 and SM261, respectively) were incubated at 25 °C or 37 °C for 4 h and imaged for GFP fluorescence. *Bar*, 10 μm.

Exo70p in all cells, except that the exocyst protein also localized to cell tips (Fig. 3*E*). We, therefore, investigated whether this complex is involved in targeting Gef3p to the septum. Exo70p is conditionally essential; when grown at 37 °C the *exo70*Δ cells die with a multiseptated phenotype. We found that Gef3p localized properly to the septum of *exo70*Δ cells both at 25 °C and 37 °C (Fig. 3*F*). A similar result was obtained with the temperature-sensitive hypomorphic *sec8-1* mutant at 37 °C, although in this case the fluorescence was accumulated intracellularly, making it more difficult to detect Gef3p in the septa (Fig. 3*F*, the *arrows* point to Gef3p fluorescence). Additionally, the localization of the exocyst components Sec6p-GFP and Sec8p-GFP was independent of the presence or absence of Gef3p (not shown). These results support the notion that septins, but not the exocyst, direct Gef3p to the growing septum.

Gef3p Interacts Physically and Functionally with Rho3p in S. pombe Cells—To study the specificity of Gef3p toward the Rho GTPases, we undertook a genetic approach. In wild-type cells the overexpression of Rho proteins is not lethal (except for Rho2p) (53), but in general it causes morphological changes and a loss of cell polarity that interferes with normal growth. Thus, if Gef3p acts through any of the GTPases it could be expected that the overexpression of this particular GTPase would be less dangerous in a *gef3*Δ background. We found that *gef3*Δ cells that expressed *rho3*$^+$ (under the control of the thiamine regulable *nmt1* promoter) grew better on a plate assay than the wild-type cells in the same conditions (Fig. 4*A*). The overexpression of *cdc42*$^+$ also produced healthier cells in the absence of *gef3*$^+$. We did not observe appreciable changes in growth among the strains due to the overexpression of the other GTPases (Fig. 4*A*). These results suggest that Gef3p could act on Rho3p and/or Cdc42p.

To confirm these results, the ORF of Gef3p (amino acids 1–525) was fused in-frame to the Gal4 transcriptional activation domain in plasmid pGAD and used as bait to screen for the interaction(s) with the Rho family proteins in a two-hybrid

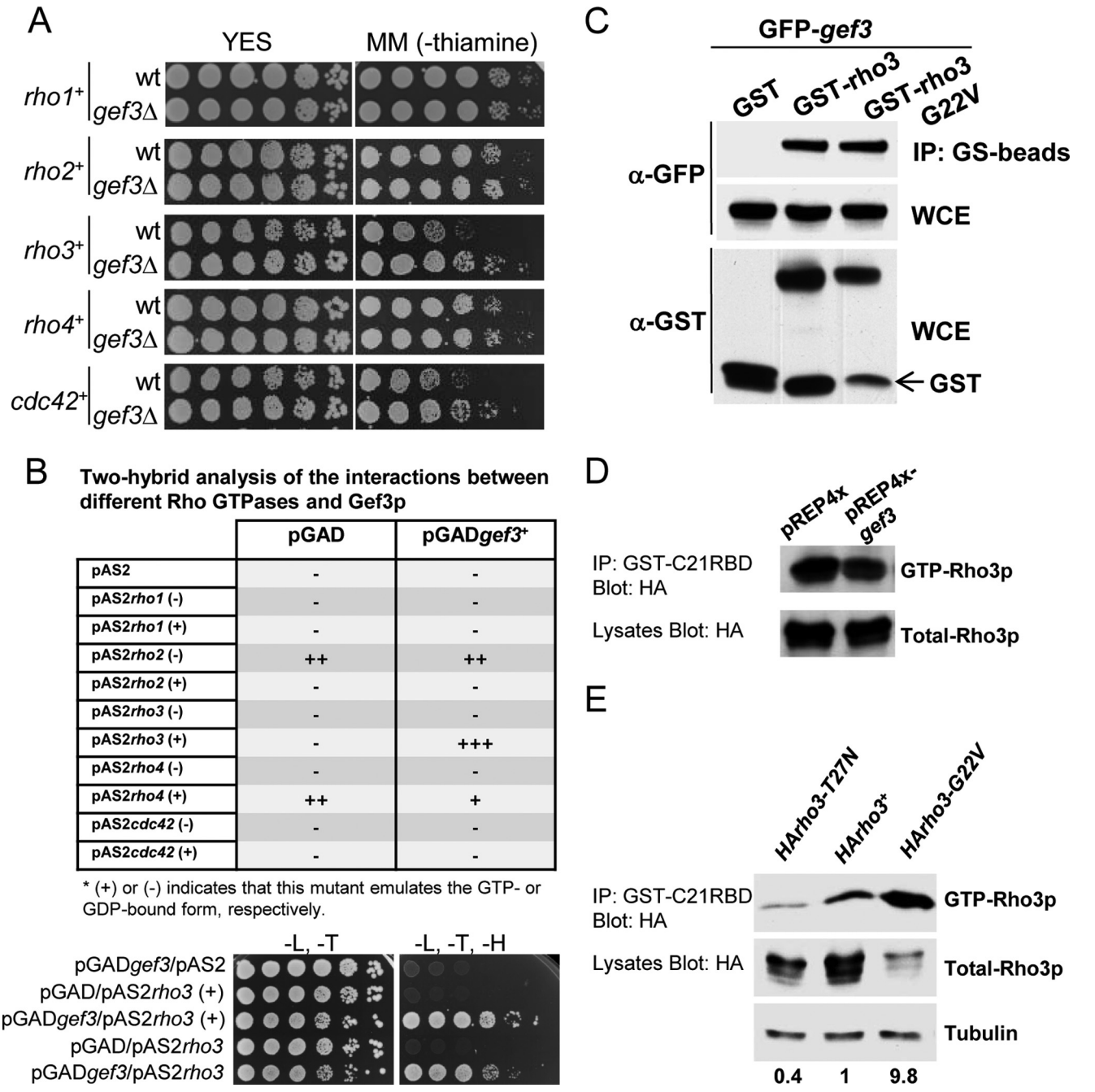

FIGURE 4. **Gef3p interacts with Rho3p.** *A*, wild-type cells (YS64) or *gef3*Δ cells (SM116) were transformed with pREP3x-*rho1*$^+$, pREP3x-*rho2*$^+$, pREP3x-*rho3*$^+$, pREP3x-*rho4*$^+$, and pREP3x-*cdc42*$^+$. Cells were spotted onto YES plates or MM (without thiamine) as serial dilutions and incubated at 28 °C for 4 days. *B*, two-hybrid analysis of the interactions between different Rho GTPases and Gef3p (*top*). Gef3p binds directly to the GTP-bound form of Rho3p (*rho3G22V*) and to the wild-type Rho3p (not modified). Growth in −Leu (*L*)/−Trp (*T*)/−His (*H*) media of yeast cotransformed with pGAD*gef3* and the empty vector pAS2 (*first row*), pAS2*rho3*(+), and the empty vector pGAD (*second row*), pGAD*gef3* and pAS2*rho3*(+) (*third row*), pAS2*rho3* and pGAD (*fourth row*), or pAS2*rho3* and pGAD*gef3* (*fifth row*) in yeast two-hybrid screenings. The results are representative of three separate co-transformation experiments. *C*, GST pulldown assay showing the interaction of Gef3p and Rho3p. Cell extracts from cells expressing GST and GFP-Gef3p, GST-Rho3p and GFP-Gef3p, and GST-Rho3p (*G22V*) and GFP-Gef3p were precipitated with glutathione beads and blotted against anti-GFP antibody. A Western blot with anti-GFP and anti-GST was performed on total extracts to visualize total GFP-Gef3p and GST-Rho3p levels (*WCE*). *D*, wild-type (YS64) cells expressing pREP4X or pREP4X-*gef3* were transformed with pREP3xHA-*rho3*. GTP-Rho3p was pulled down from the cell extracts with GST-C21RBD and blotted against 12CA5, anti-HA monoclonal antibody. Total HA-Rho3p was visualized by Western blot. *IP*, immunoblot. *E*, wild-type (MS38) cells were transformed with pREP42X-*HArho3-T27N*, pREP42X-*rho3*$^+$, and pREP42X-*HArho3-G22V*. GTP-Rho3p was pulled down from the cell extracts with GST-C21RBD and blotted against 12CA5, anti-HA monoclonal antibody. *Numbers* indicate the relationship between active Rho3p and total Rho3p normalized regarding to wild-type plasmid pREP42X-*rho3*$^+$.

assay (see "Experimental Procedures"). For each Rho protein, a point mutation that theoretically trapped the GTPase in the GTP-bound form (+) or the GDP-bound form (−) fused to the DNA binding domain was assayed (27, 43). As shown in Fig. 4*B*, Gef3p specifically interacted with the GTP-bound form of Rho3p (*rho3G22V*) but not with the GDP-bound form of Rho3p (*rho3T27N*) or with Cdc42p or indeed any of the other Rho proteins. The wild-type form of Rho3p also showed binding to

Gef3p (Fig. 4*B*). In addition, we tested two different deletion constructs of Gef3p for interaction with Rho3p, pGAD*gef3*DHΔ that lacks the DH domain and pGAD*gef3*BARΔ that lacks the BAR/IMD-like domain. Both mutant constructs showed interaction with Rho3p in a two-hybrid assay (not shown).

Next we examined whether there was interaction between Gef3p and Rho3p by co-precipitation experiments. To this end, we co-expressed GFP-epitope-tagged Gef3 protein (GFP-Gef3p) together with GST, GST-Rho3p, or GST-Rho3p (G22V) (an allele of Rho3p permanently bound to GTP) in *S. pombe* cells. As shown in Fig. 4*C*, GFP-Gef3p was found to be associated with both the wild-type Rho3p and with the GTP-bound form of Rho3p. Moreover, in a separate set of pulldown experiments using GST-RBD, we found that the amount of active Rho3p (GTP-bound Rho3p) did not increase in the strain that overexpressed Gef3p (expressed from the *nmt1* promoter, a thiamine-regulable and high expression-rate promoter) (55) as compared with the wild-type strain (Fig. 4*D*). Because GST-RBD was described to affinity-precipitate cellular GTP-RhoA (44), we further demonstrated that Rho3p binds to GST-RBD in the same way as Rho1p (the counterpart of mammalian RhoA in *S. pombe*). Extracts from wild-type cells transformed with pREP-*HA-rho3T27N* (the dominant-negative allele), pREP-*HA-rho3*$^+$ (wild-type), and pREP-*HA-rho3G22V* (the constitutively active allele) were incubated with GST-C21RBD. The experiment showed that the amount of affinity-precipitated GTP-Rho3p was different depending on the activation state. As expected the dominant negative mutant showed very little GTP-Rho3p, whereas the constitutively active allele that is always bound to GTP showed the highest levels (Fig. 4*E*). Taken together, these results suggest that Gef3p preferentially binds to the active form of Rho3p.

We then tested whether the lack of Gef3p might influence the localization and/or stability of Rho3p. Our experiments were performed with the GFP-Rho3p expressed chromosomally under its endogenous promoter.[5] As shown previously (36, 56), in wild-type cells GFP-Rho3p localized to the plasma membrane and was more intense at the division site (Fig. 5*A*). Interestingly, in *gef3*Δ cells GFP-Rho3p still localized to the plasma membrane and to the septum area (Fig. 5*A*). However, it also formed small invaginations on one or both sides of the incomplete septum (Fig. 5*A*, $n = 100$, 15% of the cells showed aberrant GFP-Rho3p). Some cells also showed similar bubbles of GFP-Rho3p at different places on the cell periphery. To ascertain whether this defect was a characteristic of GFP-Rho3p localization in *gef3*Δ cells or whether it was due to a general defect in membrane organization, we tested the localization of Psy1p-GFP in *gef3*Δ cells. The fission yeast *psy1*$^+$ gene encodes a mammalian syntaxin (t-SNARE) homolog that localizes to the plasma membrane during vegetative growth (57). Psy1p-GFP was properly localized to the plasma membrane of *gef3*Δ cells (Fig. 5*B*). Together, these results indicate that Gef3p may act as a scaffold for Rho3p, perhaps being required to concentrate active Rho3p during the early stages of septum formation when plasma membrane invagination takes place.

[5] M. A. Villar-Tajadura and P. Perez, unpublished data.

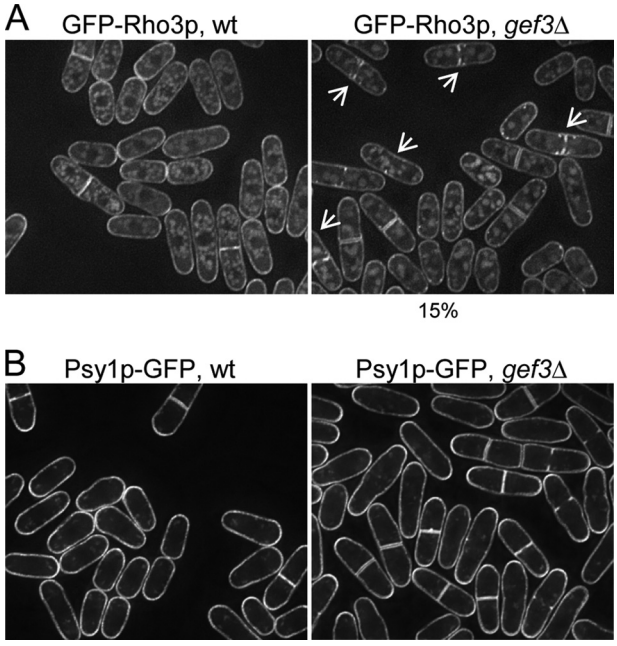

FIGURE 5. **The localization of Rho3p to the septum is disturbed in *gef3*Δ cells.** *A*, wild-type (SM242) and *gef3*Δ (SM594) cells expressing a functional, chromosomal GFP-Rho3p from the endogenous promoter were grown in YES medium at 28 °C and imaged for fluorescence. Maximum projection images are shown. *B*, wild-type (EM83) and *gef3*Δ (EM256) cells expressing a functional, chromosomal Psy1p-GFP were grown in YES medium at 28 °C and imaged for fluorescence. Maximum projection images are shown.

*Loss of Gef3p Shows Genetic Interactions with Exocyst Mutants, apm1*Δ *Mutants, and Formin Mutants*—The above results suggested that Gef3p was more related to Rho3p than to any of the other GTPases of the Rho family. Accordingly, we deleted *gef3*$^+$ in *rho3*Δ cells to conduct epistasis experiments. The double mutant *gef3*Δ*rho3*Δ grew as well as the single mutant *rho3*Δ in a temperature range between 25 °C and 35 °C, whereas neither of them was able to grow at 37 °C (Fig. 6*A*), suggesting that Gef3p and Rho3p could act in the same pathway. We then wondered which of the Rho3p functions might be specifically affected by Gef3p. In *S. pombe*, the overproduction of Rho3p compensates the abnormal elongated multicellular phenotype of *sec8-1* and *exo70*Δ exocyst mutants, and *rho3*Δ shows strong negative interactions with *sec8-1* and *exo70*Δ. Accordingly, we analyzed whether the exocyst was functionally related to Gef3p. The overproduction of Gef3p did not suppress the thermosensitive phenotype of the *sec8-1* mutant (not shown). However, the *sec8-1 gef3*Δ double-mutant cells showed a severe growth defect. They did not form colonies detectable at 35 °C, a cell growth-permissive temperature for each single mutant (Fig. 6*B*). Although *gef3*Δ and *sec8-1* showed a mild cell separation defect at 25 °C (Fig. 6*B*), this phenotype was exacerbated in the *sec8-1 gef3*Δ double mutant, most cells arresting with multiple septa (Fig. 6*B*) and similar to the *sec8-1* phenotype at 37 °C (28). In addition, a genetic interaction was found between *gef3*Δ and *exo70*Δ (not shown). Rho3p regulates secretion by influencing membrane trafficking in cooperation with Apm1p (34). Therefore, we also entertained the possibility of the existence of a functional link between Gef3p and genes encoding adaptin. We found that *gef3*Δ*apm1*Δ cells grew at 25 °C but did not form colonies detectable at 35 °C (a cell growth-permissive temper-

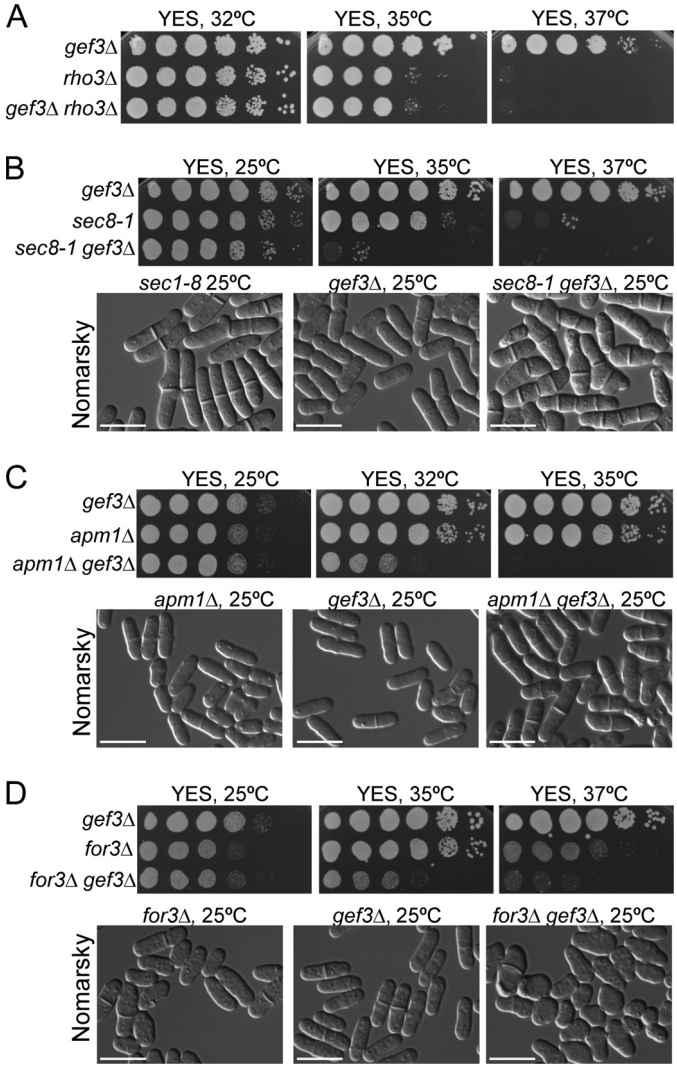

FIGURE 6. **Loss of Gef3p shows genetic interactions with exocyst mutants, adaptin mutants, and formin mutants.** *A*, *gef3*Δ*rho3*Δ behaved like *rho3*Δ cells in their ability to grow at high temperatures. To compare the relative growth rates, equal numbers of *gef3*Δ (SM176), *rho3*Δ (PPG3740), and *gef3*Δ*rho3*Δ (EM257) cells were diluted (8×10^4 cells in the *left rows* and then 4×10^4, 2×10^4, 2×10^3, 2×10^2, and 2×10^1 in each subsequent spot) and spotted onto YES plates. Colony formation was analyzed after 3 days at 32, 35, and 37 °C. *B*, the *gef3*Δ *sec8-1* double-mutant strain was unable to form colonies at 35 °C. To compare relative growth rates, *gef3*Δ (SM176), *sec8-1* (MBY887), and *gef3*Δ *sec8-1* (SM226) cells were spotted onto YES plates as above and incubated at 25, 35, and 37 °C for 3 days (*upper panel*). *gef3*Δ, *sec8-1*, and *gef3*Δ*sec8-1* cells were observed directly in YES liquid medium at 25 °C by differential interference-contrast microscopy (*lower panel*). *C*, loss of both $gef3^+$ and $apm1^+$ results in failure to grow at 32 and 35 °C. To compare the growth rates, *gef3*Δ (SM176), *apm1*Δ (SM708), and *gef3*Δ*apm1*Δ (SM721), cells were spotted onto YES plates and incubated for 3 days at different temperatures (*upper panels*). Differential interference-contrast photographs of *gef3*Δ, *apm1*Δ, and *gef3*Δ *apm1*Δ cells grown in YES liquid medium at 25 °C (*lower panels*). *D*, *gef3*Δ*for3*Δ double-mutant cells fail to polarize growth. *gef3*Δ (SM176), *for3*Δ (PPG2567), and *gef3*Δ *for3*Δ (SM300) cells were diluted, spotted onto YES plates, and incubated at 25, 35, and 37 °C (*upper panels*). Differential interference-contrast photographs of *gef3*Δ, *for3*Δ, and *gef3*Δ*for3*Δ cells grown at 25 °C (*lower panels*). *Bar*, 10 μm.

ature for each single mutant) (Fig. 6*C*). Moreover, even at 25 °C >90% of the cells showed 1 septum. Thus, Gef3p and Apm1p interact genetically to promote cell growth at high temperature.

Finally, we explored whether Gef3p might be involved in the Rho3p function in polarity. Rho3p binds to For3p, which is the *S. pombe* ortholog of formin, and the *rho3*Δ*for3*Δ double-null cells showed defects that were more severe than those seen in each of the single null cells; that is, round cells appeared (36). Because Gef3p binds to the active form of Rho3p, we speculated that in *gef3*Δ cells active Rho3p is not properly concentrated and that polarity would be compromised if actin cables were absent due to the deletion of For3p. To examine this possibility, For3p was deleted from the *gef3*Δ mutant, and the phenotype of the resulting double mutant was assessed. A synthetic cell growth defect was observed at 35 °C, and this was more severe at 37 °C (Fig. 6*D*). Moreover, the double-mutant cells frequently showed a lemon-like shape, similar to *rho3*Δ*for3*Δ cells and swelled from the middle even at 25 °C (Fig. 6*D*). This phenotype like the one reported for *pob1-664* mutant cells at the restrictive temperature (37, 40). Thus, the results suggest that the function of Gef3p is important for Rho3p to control secretion, especially if one of the two molecular systems involved in vesicle-trafficking, namely vesicle tethering and vesicle transport, is also affected.

DISCUSSION

GEF activation of Rho GTPases occurs through the serial formation of macromolecular complexes at precise points in time and space that are currently incompletely understood. Here we studied a Rho-GEF, termed Gef3p, which like other Rho-GEFs contains a DH but lacks the pleckstrin homology domain that is required for most Rho-GEFs to localize to the membrane (59). Instead, at the C terminus Gef3p carries a putative BAR/IMD-like domain. The IMD (IRSp53 and MIM (missing in metastases) homology domain) is an I-BAR or inverse BAR domain that binds to the membrane through its convex surface. IMD domains are involved in plasma membrane deformation, producing protrusions (filopodia and lamellipodia) (60, 61).

In this study we assigned a function to Gef3p that was directly related to the assembly of Rho3p GTPase to the septum. Gef3p interacts functionally with Rho3p, and the loss of Gef3p aggravates the phenotypes of exocyst mutants and formin mutants, similar to what has been described previously for the loss of Rho3p (28, 36). Biochemical and genetic evidence suggests that Gef3p interacts with Rho3p, although it does not seem to promote nucleotide exchange of the GTPase. Gef3p bound to the active form of Rho3p but not to other Rho proteins (either GDP- or GTP-bound) in a two-hybrid assay. Moreover, wild-type Rho3p and GTP-bound Rho3p coprecipitated with Gef3p. The GDP/GTP cycle is highly regulated by GEFs, which induce the release of the bound GDP for replacement by the more abundant GTP. As a result, GEFs usually accelerate the exchange reaction by several orders of magnitude (12, 13). Despite this, here we observed that high levels of Gef3p did not raise the level of GTP-Rho3p *in vivo*. We also tested the effect of the overexpression of Gef3p on the GTP-bound levels of the other GTPases, from Rho1p to Rho4p and Cdc42p, with negative results. Thus, Gef3p apparently does not activate Rho3p, which could explain why the overexpression of Rho3p, but not that of Gef3p, suppressed the thermosensitive phenotype of the *sec8-1* mutants (36) or *amp1*Δ mutants (34) (not shown). Rho3p binds to Gef3p lacking its DH domain in a two-hybrid assay, suggesting again that Gef3p is not working as a GEF for

Rho3p. From our results it is likely that both, the DH and BAR/IMD-like domains, could participate in binding. In this sense, a series of BAR domain-containing proteins have been characterized that are linked to Rho GTPase signaling pathways (62). BAR domains play important roles in the targeting of proteins to specific regions within the plasma membrane where actin remodeling is necessary. At these sites, BAR-domain proteins can control Rho GTPase activity either by regulating the activation status of Rho GTPases or by linking Rho GTPases to their upstream activators or to their downstream effectors (45, 61).

The interaction Gef3p/Rho3p is not unique; in certain circumstances allosteric interactions of the GEF with either the GTPase itself or with its effectors can create an environment that seems to sustain the GTPase activity without modifying the nucleotide binding state of the GTPase. The Gef3p/Rho3p interaction might be required for stabilization of the active form of Rho3p at the septum. GFP-Rho3p showed a uniform membrane distribution, and we failed to observe important differences between the wild-type and *gef3*Δ cells in the localization of Rho3p to the septum. However, in *gef3*Δ, GFP-Rho3p was often invaginated in the wrong place, surrounding immature septa. This suggests that Gef3p binding to active Rho3p might stabilize the protein, promoting its accumulation at the contractile actomyosin ring/invaginated membrane interface. Alternatively, Gef3p may convey active Rho3p to a specific platform to become part of a higher-order complex. Here, we noted that Gef3p localized to the cell division site after septins had been deposited and that it required septins for localization. Septins are filament-forming (GTP-binding) proteins that assemble at the division site. In many systems they appear to serve as scaffolds and diffusion barriers for other proteins, and they are important for cytokinesis (50, 63–65). Recent findings suggest that septins regulate membrane traffic or membrane stability (66, 67). Septins could cross-link and corral membrane domains enriched in particular phosphoinositides, blocking the lateral diffusion of membrane proteins and deforming or rigidifying the cell membrane (54, 68, 69). In fission yeast septins are not essential for cell viability, and mutants display a variable delay in separation of the daughter cells, suggesting that septins play some role(s) in the proper completion of the septum or in subsequent processes necessary for cell separation (50, 54, 58, 68). Rho3p is not essential for viability, but cells depleted of Rho3p were elongated and multiseptated, and they accumulated putative secretory vesicles at high temperature (28, 34, 36, 37). Thus, the loss of function of both pathways produces similar cytokinetic defects. In *mid2*Δ and *spn* mutants, failure in septin ring assembly impairs the formation of the Gef3p ring and may culminate in perturbing Rho3p function in the medial region. Consistent with this idea, we found that a combination of a defective septin ring (*mid2*Δ) with a mutation in the adaptin complex (*apm1*Δ), an effector of Rho3p, was lethal above 32 °C; this phenotype is almost identical to the one seen in *gef3*Δ*apm1*Δ cells (Fig. 6*C*). As expected, *mid2*Δ*gef3*Δ cells grew well at all temperatures. Together, these results suggest that one of the functions of the septin ring in *S. pombe* could be to act as a positional cue for the targeting of active Rho3p.

*gef3*Δ cells grew similarly to wild-type cells. However, a deletion of Gef3p caused a small delay in cell-cell separation, suggesting a role for the protein in cytokinesis. Curiously, the interaction with other GEFs may help to understand its role in septum dynamics. The *gef3*Δ cytokinesis phenotype was aggravated by the deletion of Gef1p (a Cdc42-GEF), producing highly multiseptated cells (Fig. 1*E*). However, the elimination of Gef3p suppressed hypersensitivity to NaF and lysis in *ehs2-1* cells mutated in Rgf3p (a Rho1p-GEF). Thus, the most attractive hypothesis to explain the data is that Gef3p would be involved in a pathway whose function normally complements that of Cdc42p. In addition, the Gef3p/Rho3p pathway might negatively modulate Rho1p signaling, and hence its absence would raise the level of Rho1p, which would help to correct the damage. Our results are consistent with the possibility that Gef3p/Rho3p could function redundantly with the Cdc42p pathway in cytokinesis. Cdc42p is likely to form the most upstream polarizing cue and activates the formin For3p for the assembly of polarized actin cables. This interaction is facilitated by Pob1p (36, 38–40). The *pob1-664* mutant shows an accumulation of secretory vesicles and a loss of functional actin cables, and both phenotypes are suppressed by Rho3p (37).

Our results suggest that Gef3p functions by stabilizing active Rho3p and facilitating the interaction of Rho3p with its effectors during the early steps of septum synthesis. This is shown by the fact that a lack of Gef3p produced defects similar to the deletion of Rho3p when combined with mutants in the exocyst and formins (31). The simultaneous mutation of *gef3*$^+$ and *sec8*$^+$ and *gef3*$^+$ and *apm1*$^+$, both genes encoding proteins involved in secretion, afforded cells with strong defects in septation. In addition, a severe synthetic cell growth defect in polarity was observed in the *gef3*Δ*for3*Δ double mutants. These cells frequently showed a lemon-like shape similar to *pob1-664* and misslocalized septa (Fig. 6*D*). As the Gef3p and Rho3p are both required for polar growth in the absence of actin cables (this work and Ref. 36), this complex could provide key spatial information to identify zones of growth, a redundant function related to the master role of Cdc42p in polarized exocytosis. It is possible that the septins that localize Gef3p also play a role in this process.

In conclusion, we observed that the putative Rho-GEF Gef3p binds to active Rho3p and localizes to the septin ring, providing a platform for GTPase function during septum assembly and/or degradation. The Gef3p/Rho3p interaction contributes to downstream events in the secretory pathway redundantly with the two autonomous "morphogenetic modules": the exocyst and the actin cable machinery.

Acknowledgments—We thank P. Perez, P. M. Coll, H. Valdivieso, J. C. Ribas, and C. Rodriguez-Vazquez de Aldana from the IBFG, Spain, F. Chang from Columbia University, M. Balasubramanian from the Mechanobiology Institute, Singapore, and J. Bähler from Wellcome Trust UK for providing plasmids and strains. We recognize P. Bolaños for initiating this work. Text was revised by N. Skinner. Instituto de Biología Funcional y Genómica acknowledges the institutional support granted by the Ramón Areces Foundation during 2011 and 2012.

REFERENCES

1. Pollard, T. D. (2010) Mechanics of cytokinesis in eukaryotes. *Curr. Opin. Cell Biol.* **22,** 50–56

2. Balasubramanian, M. K., Srinivasan, R., Huang, Y., and Ng, K.-H. (2012) Comparing contractile apparatus-driven cytokinesis mechanisms across kingdoms. *Cytoskeleton* **69,** 942–956
3. Krapp, A., and Simanis, V. (2008) An overview of the fission yeast septation initiation network (SIN). *Biochem. Soc. Trans.* **36,** 411–415
4. Bathe, M., and Chang, F. (2010) Cytokinesis and the contractile ring in fission yeast: towards a system-level understanding. *Trends Microbiol.* **18,** 38–45
5. Goyal, A., Takaine, M., Simanis, V., and Nakano, K. (2011) Dividing the spoils of growth and the cell cycle: the fission yeast as a model for the study of cytokinesis. *Cytoskeleton* **68,** 69–88
6. Pollard, T. D., and Wu, J. Q. (2010) Understanding cytokinesis: lessons from fission yeast. *Nat. Rev. Mol. Cell Biol.* **11,** 149–155
7. Roncero, C., and Sánchez, Y. (2010) Cell separation and the maintenance of cell integrity during cytokinesis in yeast: the assembly of a septum. *Yeast* **27,** 521–530
8. Sipiczki, M. (2007) Splitting of the fission yeast septum. *FEMS Yeast Res.* **7,** 761–770
9. Wolfe, B. A., and Glotzer, M. (2009) Single cells (put a ring on it). *Genes Dev.* **23,** 896–901
10. Yoshida, S., Bartolini, S., and Pellman, D. (2009) Mechanisms for concentrating Rho1 during cytokinesis. *Genes Dev.* **23,** 810–823
11. Yoshida, S., Kono, K., Lowery, D. M., Bartolini, S., Yaffe, M. B., Ohya, Y., and Pellman, D. (2006) Polo-like kinase Cdc5 controls the local activation of Rho1 to promote cytokinesis. *Science* **313,** 108–111
12. Bos, J. L., Rehmann, H., and Wittinghofer, A. (2007) GEFs and GAPs: critical elements in the control of small G proteins. *Cell* **129,** 865–877
13. Buchsbaum, R. J. (2007) Rho activation at a glance. *J. Cell Sci.* **120,** 1149–1152
14. Rossman, K. L., Der, C. J., and Sondek, J. (2005) GEF means go: turning on Rho GTPases with guanine nucleotide-exchange factors. *Nat. Rev. Mol. Cell Biol.* **6,** 167–180
15. Schmidt, A., and Hall, A. (2002) Guanine nucleotide exchange factors for Rho GTPases: turning on the switch. *Genes Dev.* **16,** 1587–1609
16. García, P., Tajadura, V., García, I., and Sánchez, Y. (2006b) Role of Rho GTPses and Rho-GEFs in the regulation of cell shape and integrity in fission yeast. *Yeast* **23,** 1031–1043
17. Iwaki, N., Karatsu, K., and Miyamoto, M. (2003) Role of guanine nucleotide exchange factors for Rho family GTPases in the regulation of cell morphology and actin cytoskeleton in fission yeast. *Biochem. Biophys. Res. Commun.* **312,** 414–420
18. Perez, P., and Rincón, S. A. (2010) Rho GTPases: regulation of cell polarity and growth in yeasts. *Biochem. J.* **426,** 243–253
19. Hirota, K., Tanaka, K., Ohta, K., and Yamamoto, M. (2003) Gef1p and Scd1p, the two GDP-GTP exchange factors for Cdc42p, form a ring structure that shrinks during cytokinesis in *Schizosaccharomyces pombe*. *Mol. Biol. Cell* **14,** 3617–3627
20. Coll, P. M., Rincon, S. A., Izquierdo, R. A., and Perez, P. (2007) Hob3p, the fission yeast ortholog of human BIN3, localizes Cdc42p to the division site and regulates cytokinesis. *EMBO J.* **26,** 1865–1877
21. Ye, Y., Lee, I.-J., Runged, K. W., and Wu, J.-Q. (2012) Roles of putative Rho-GEF Gef2 in division-site positioning and contractile-ring function in fission yeast cytokinesis. *Mol. Biol. Cell* **23,** 1181–1195
22. García, P., García, I., Marcos, F., de Garibay, G. R., and Sánchez, Y. (2009b) Fission yeast Rgf2p is a Rho1p guanine nucleotide exchange factor required for spore wall maturation and for the maintenance of cell integrity in the absence of Rgf1p. *Genetics* **181,** 1321–1334
23. García, P., Tajadura, V., García, I., and Sánchez, Y. (2006a) Rgf1p is a specific Rho1-GEF that coordinates cell polarization with cell wall biogenesis in fission yeast. *Mol. Biol. Cell* **17,** 1620–1631
24. Garcia, P., Tajadura, V., and Sanchez, Y. (2009a) The Rho1p exchange factor Rgf1p signals upstream from the Pmk1 mitogen-activated protein kinase pathway in fission yeast. *Mol. Biol. Cell* **20,** 721–731
25. Mutoh, T., Nakano, K., and Mabuchi, I. (2005) Rho1-GEFs Rgf1 and Rgf2 re involved in formation of cell wall and septum, while Rgf3 is involved in cytokinesis in fission yeast. *Genes Cells* **10,** 1189–1202
26. Morrell-Falvey, J. L., Ren, L., Feoktistova, A., Haese, G. D., and Gould, K. L. (2005) Cell wall remodeling at the fission yeast cell division site requires the Rho-GEF Rgf3p. *J. Cell Sci.* **118,** 5563–5573
27. Tajadura, V., García, B., García, I., García, P., and Sánchez, Y. (2004) *Schizosaccharomyces pombe* Rgf3p is a specific Rho1 GEF that regulates cell wall β-glucan biosynthesis through the GTPase Rho1p. *J. Cell Sci.* **117,** 6163–6174
28. Wang, H., Tang, X., and Balasubramanian, M. K. (2003) Rho3p regulates cell separation by modulating exocyst function in *Schizosaccharomyces pombe*. *Genetics* **164,** 1323–1331
29. TerBush, D. R., Maurice, T., Roth, D., and Novick, P. (1996) The exocyst a multiprotein complex required for exocytosis in *Saccharomyces cerevisiae*. *EMBO J.* **15,** 6483–6494
30. Heider, M. R., and Munson, M. (2012) Exorcising the exocyst complex. *Traffic* **13,** 898–907
31. Bendezú, F. O., and Martin, S. G. (2011) Actin cables and the exocyst form two independent morphogenesis pathways in the fission yeast. *Mol. Biol. Cell* **22,** 44–53
32. Bendezú, F. O., Vincenzetti, V., and Martin, S. G. (2012) Fission yeast Sec3 and Exo70 are transported on actin cables and localize the exocyst complex to cell poles. *Plos ONE* **7,** e40248
33. Estravís, M., Rincón, S. A., Santos, B., and Pérez, P. (2011) Cdc42 regulates multiple membrane traffic events in fission yeast. *Traffic* **12,** 1744–1758
34. Kita, A., Li, C., Yu, Y., Umeda, N., Doi, A., Yasuda, M., Ishiwata, S., Taga, A., Horiuchi, Y., and Sugiura, R. (2011) Role of the small GTPase Rho3 in Golgi/endosome trafficking through functional interaction with adaptin in Fission Yeast. *Plos ONE* **6,** e16842
35. Yu, Y., Li, C., Kita, A., Katayama, Y., Kubouchi, K., Udo, M., Imanaka, Y., Ueda, S., Masuko, T., and Sugiura, R. (2013) Sip1, an AP-1 accessory protein in fission yeast, is required for localization of Rho3 GTPase. *Plos ONE* **8,** e68488
36. Nakano, K., Imai, J., Arai, R., Toh-E, A., and Matsui, Y., and Mabuchi, I. (2002) The small GTPase Rho3 and the diaphanous/formin For3 function in polarized cell growth in fission yeast. *J. Cell Sci.* **115,** 4629–4639
37. Nakano, K., Toya, M., Yoneda, A., Asami, I. Y., and Yamashita, A., Kamasawa, N., Osumi, M., and Yamamoto, M. (2011) Pob1 ensures cylindrical cell shape by coupling two distinct Rho signaling events during secretory vesicle targeting. *Traffic* **12,** 726–739
38. Feierbach, B., and Chang, F. (2001) Roles of the fission yeast formin For3 in cell polarity, actin cable formation, and symmetric cell division. *Curr. Biol.* **11,** 1656–1665
39. Martin, S. G., Rincón, S. A., Basu, R., Pérez, P., and Chang, F. (2007) Regulation of the formin for3p by cdc42p and bud6p. *Mol. Biol. Cell* **18,** 4155–4167
40. Rincón, S. A., Ye, Y., Villar-Tajadura, M. A., Santos, B., Martin, S. G., and Pérez, P. (2009) Pob1 participates in the Cdc42 regulation of fission yeast actin cytoskeleton. *Mol. Biol. Cell* **20,** 4390–4399
41. Moreno, S., Klar, A., and Nurse, P. (1991) Molecular genetic analysis of fission yeast *Schizosaccharomyces pombe*. *Methods Enzymol.* **194,** 795–823
42. Shaner, N. C., Steinbach, P. A., and Tsien, R. Y. (2005) A guide to choosing fluorescent proteins. *Nat. Methods* **2,** 905–909
43. Coll, P. M., Trillo, Y., Ametzazurra, A., and Perez, P. (2003) Gef1p, a new guanine nucleotide exchange factor for Cdc42p, regulates polarity in *Schizosaccharomyces pombe*. *Mol. Biol. Cell* **14,** 313–323
44. Ren, X. D., Kiosses, W. B., and Schwartz, M. A. (1999) Regulation of the small GTP-binding protein Rho by cell adhesion and the cytoskeleton. *EMBO J.* **18,** 578–585
45. Habermann, B. (2004) The BAR-domain family of proteins: a case of bending and binding? *EMBO Rep.* **5,** 250–255
46. Aspenström, P. (2009) Roles of F-BAR/PCH proteins in the regulation of membrane dynamics and actin reorganization. *Int. Rev. Cell Mol. Biol.* **272,** 1–31
47. Laporte, D., Coffman, V. C,, Lee, I. -J., and Wu, J.-Q. (2011) Assembly and architecture of precursor nodes during fission yeast cytokinesis. *J. Cell Biol.* **192,** 1005–1021
48. Cortés, J. C., Konomi, M., Martins, I. M., Muñoz, J., Moreno, M. B., Osumi, M., Durán, A., and Ribas, J. C. (2007) The (1,3)β-D-glucan synthase subunit Bgs1p is responsible for the fission yeast primary septum formation. *Mol. Microbiol.* **65,** 201–217

49. Berlin, A., Paoletti, A., and Chang, F. (2003) Mid2p stabilizes septin rings during cytokinesis in fission yeast. *J. Cell Biol.* **160,** 1083–1092
50. Longtine, M. S., DeMarini, D. J., Valencik, M. L., Al-Awar, O. S., and Fares, H., De Virgilio, C., and Pringle, J. R. (1996) The septins: roles in cytokinesis and other processes. *Curr. Opin. Cell Biol.* **8,** 106–119
51. Tasto, J. J., Morrell, J. L., and Gould, K. L. (2003) An anillin homologue, Mid2p, acts during fission yeast cytokinesis to organize the septin ring and promote cell separation. *J. Cell Biol.* **160,** 1093–1103
52. He, B., and Guo, W. (2009) The exocyst complex in polarized exocytosis. *Curr. Opin. Cell Biol.* **21,** 537–542
53. Hirata, D., Nakano, K., Fukui, M., Takenaka, H., Miyakawa, T., and Mabuchi, I. (1998) Genes that cause aberrant cell morphology by overexpression in fission yeast: a role for a small GTP-binding protein Rho2 in cell morphogenesis. *J. Cell Sci.* **111,** 149–159
54. Martín-Cuadrado, A. B., Morrell, J. L., Konomi, M., An, H., Petit, C., Osumi, M., Balasubramanian, M., Gould, K. L., Del Rey, F., and de Aldana, C. R. (2005) Role of septins and the exocyst complex in the function of hydrolytic enzymes responsible for fission yeast cell separation. *Mol. Biol. Cell* **16,** 4867–4881
55. Forsburg, S. L. (1993) Comparison of *Schizosaccharomyces pombe* expression systems. *Nucleic Acids Res.* **21,** 2955–2956
56. Wang, H., Tang, X., Liu, J., Trautmann, S., Balasundaram, D., McCollum, D., and Balasubramanian, M. K. (2002) The multiprotein exocyst complex is essentail for cell separation in *Schizosaccharomyces pombe*. *Mol. Biol. Cell* **13,** 515–529
57. Nakamura, T., Nakamura-Kubo, M., Hirata, A., and Shimoda, C. (2001) The *Schizosaccharomyces pombe spo3*$^+$ gene is required for assembly of the forespore membrane and genetically interacts with *psy1*$^+$-encoding syntaxin-like protein. *Mol. Biol. Cell* **12,** 3955–3972
58. Wu, J.-Q., Ye, Y., Wang, N., Pollard, T. D., and Pringle, J. R. (2010) Cooperation between the septins and the actomyosin ring and role of a cell-integrity pathway during cell division in fission yeast. *Genetics* **186,** 897–915
59. Rossman, K. L., and Sondek, J. (2005b) Larger than Dbl: new structural insights into RhoA activation. *Trends Biochem. Sci.* **30,** 163–165
60. Suetsugu, S., Toyooka, K., and Senju, Y. (2010) Subcellular membrane curvature mediated by the BAR domain superfamily proteins. *Semin. Cell Dev. Biol.* **21,** 340–349
61. Frost, A., Unger, V. M., and De Camilli, P. (2009) The BAR domain superfamily: membrane-molding macromolecules. *Cell* **137,** 191–196
62. de Kreuk, B. J., and Hordijk, P. L. (2012) Control of Rho GTPase function by BAR-domains. *Small GTPases* **3,** 45–52
63. Caudron, F., and Barral, Y. (2009) Septins and the lateral compartmentalization of eukaryotic membranes. *Dev. Cell* **16,** 493–506
64. Gladfelter, A. S., Pringle, J. R., and Lew, D. J. (2001) The septin cortex at the yeast mother-bud neck. *Curr. Opin. Microbiol.* **4,** 681–689
65. Barral, Y. (2008) Yeast septins: a cortical organizer. Chapter 4, in *The Septins* (Hall, P. A., Russell, S. E. H., and Pringle, J. R., eds) pp. 101–125, Wiley Blackwell, London
66. Joo, E., Tsang, C. W., and Trimble, W. S. (2005) Septins: traffic control at the cytokinesis intersection. *Traffic* **6,** 626–634
67. Spiliotis, E. T., and Gladfelter, A. S. (2012) Spatial guidance of cell asymmetry: septin GTPases show the way. *Traffic* **13,** 195–203
68. An, H., Morrell, J. L., Jennings, J. L., Link, A. J., and Gould, K. L. (2004) Requirements of fission yeast septins for complex formation, localization, and function. *Mol. Biol. Cell* **15,** 5551–5564
69. Zhang, J., Kong, C., Xie, H., McPherson, P. S., Grinstein, S., and Trimble, W. S. (1999) Phosphatidylinositol polyphosphate binding to the mammalian septin H5 is modulated by GTP. *Curr. Biol.* **9,** 1458–1467